Article

Experimental Analysis on a Spray Hydrocooler with Cold Energy Storage for Litchi

Hao Huang [1], Enli Lv [1,2,] *, Huazhong Lu [1,2] and Jiaming Guo [1,2]

[1] College of Engineering, South China Agricultural University, Guangzhou 510642, China
[2] Key Laboratory of Key Technology on Agricultural Machine and Equipment, Ministry of Education, Guangzhou 510642, China
* Correspondence: fanchen324216@163.com; Tel.: +86 135-6000-8066

Abstract: The shortage of precooling equipment in litchi producing regions could lead to a high loss rate, poor quality of litchis. It is urgent to develop a portable precooling device for litchi producing regions. In this study, a novel spray hydrocooler with thermal energy storage (TES) were designed, fabricated, and tested. A simple mathematical model of TES capacity, ice coil thermal resistance and refrigeration system was employed to determine hydrocooler parameters. Then designed the structure of the spray hydrocooler. Maximum charging test was implemented with full TES capacity and litchi spray hydrocooling experiments were carried out at different charging times, spray flow rate, and litchi load with one-third TES capacity. Results showed that: (1) the spray hydrocooler allows for the rapid and effective precooling of litchis; (2) the hydrocooler can precool 299 kg litchis with one-third TES storage, meet the precooling requirements; (3) the effective TES capacity achieved 1.25×10^8 J at the maximum TES capacity of the hydrocooler, while the energy efficiency ratio (EER) is 2; (4) the precooling capacity was maximum and the average power consumption was minimum when the litchi load was 23 kg and the spray flow rate was 30 L min^{-1}. Longer charging time is the most important factor in increasing precooling capacity and reducing average power consumption.

Keywords: Thermal energy storage; Hydrocooler; Heat transfer; Refrigeration; Litchi

1. Introduction

Litchi (*Litchi chinensis*), a perishable fruit, is loved by people worldwide. and China contributes to 60% of the world's production[1]. Litchi mainly matures in summer and have a high temperature of flesh and skin, which contain large amounts of field heat after harvest[2]. In the postharvest environment water lost from litchi due to transpiration is not well-replenished causing rapid deterioration[3]. Loss of litchis occur due to a lack of proper and timely postharvest treatment [4]. Applying a cold treatment during postharvest can effectively lessen respiration, inhibit microbial growth and reduce enzyme activity in fruits and vegetables[5-6].

Precooling is the first step to rapidly cool down the harvested products to the required temperature by using a low-temperature medium to remove heat. As such, precooling is required immediately after harvest to eliminate field heat, to significantly extend the shelf life and improve commodity quality[7]. There are four methods commonly used for precooling of various fruits and vegetables[8-9]. Forced-air cooling requires several hours and can easily lead to the formation of hot spots and water loss[10]. Ice cooling can cause uneven cooling, insufficient cooling, frostbite, soft rots on products and increase transportation costs[11-12]. Vacuum cooling leads to water loss and is not suitable for products with a low surface to volume rate[13-14]. Hydrocooling could reduce water loss, avoid skin softening of crops and is about 2–15 times faster than forced-air cooling under similar conditions[15-16]. Litchi, apple, cherry, sweet corn, radishes, Barhee dates, and carrots are precooled successfully using hydrocooling[8,17-18,19].

At present, postharvest litchi precooling treatment is inadequate[20]. After being picked, most litchis are transported and sold with ice bags. However, litchi lose their commercial value by

Preprints (www.preprints.org) | NOT PEER-REVIEWED | Posted: 13 June 2023 doi:10.20944/preprints202306.0866.v1

browning and decaying quickly[21]. Few litchis are transported to litchi processing enterprises and immersed in ice water or cold water for precooling. Precooling facilities are generally far away from litchi production[20]. Due to the costs of transportation and processing, litchi precooling costs are high. In addition, ice water immersion precooling is prone to overcooling or undercooling[22]. In China, the existing precooling equipment in litchi producing regions is limited to laboratory research. There is no precooling equipment that can precool litchis timely and quickly and meet the precooling demand of litchi producer.

TES systems can store either heat or cold energy[23]. Energy can be charged, stored and discharged on a daily, weekly, seasonal or annual basis[24]. It can shift energy usage from the peak to the off-peak periods, and shift the energy to areas faced with a shortage. In this study, a spray hydrocooling device using TES technology was newly designed and fabricated. TES performance and the precooler's spray cooling performance were investigated under different test conditions. The spray hydrocooling device was charged at night and suitable for litchi producing areas without power supply. It is small in size and light in weight, and can be easily transferred to litchi producing regions.

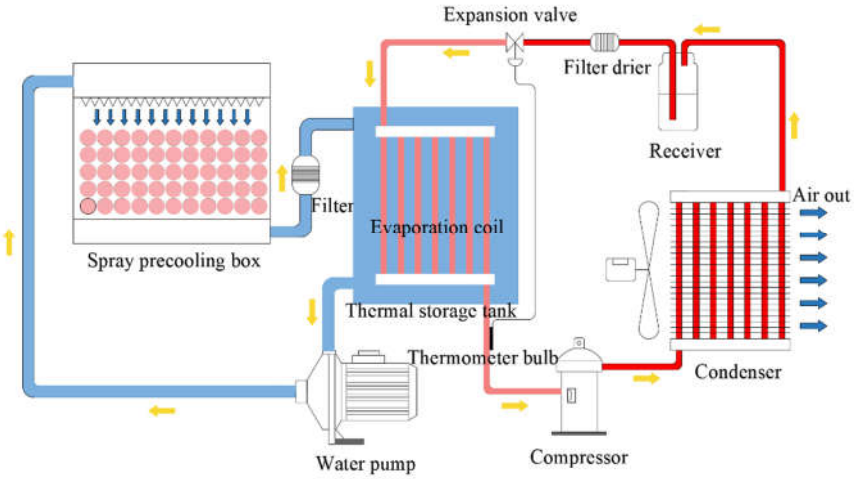

Figure 1. Operation principle diagram of the spray hydrocooler.

2. Mathematical model of the hydrocooler

The usual precooler is precooling during refrigeration with the refrigeration capacity determining the precooling rate of fruits and vegetables. The precooler in this study provides energy source from TES. The refrigerator runs when cooling is idle, and the thermal energy is stored in the TES tank. During precooling, the energy in the TES tank is released to cool fruits and vegetables. The hydrocooler is mainly composed of the TES system and spray hydrocooling system (Figure 1). The evaporation coil is located in the TES box, which is filled with water. During charging, the thermal energy is stored as cold water and ice. During precooling, the cold water of TES tank is pumped to the precooling box, and sprayed on the surface of fruits and vegetables through the spray device of the precooling box. The temperature of fruits and vegetables is reduced due to the heat exchange between cold water and fruits, vegetables. The used water flows back to the TES tank and exchanges heat with the ice in the TES tank. The precooling capacity of fruits and vegetables is determined by the thermal energy stored in the TES tank, the thermal insulation characteristics of the device and the thermodynamic properties of fruits and vegetables. Therefore, it is necessary to establish the mathematical model for the precooler to calculate the key design parameters such as TES capacity in order to the precooling demand and hence design and manufacture a suitable device.

Preprints (www.preprints.org) | NOT PEER-REVIEWED | Posted: 13 June 2023 doi:10.20944/preprints202306.0866.v1

Nomenclature

	area, m^2
A	specific heat, J kg^{-1} K^{-1}
c	latent heat, J kg^{-1}
C	diameter, m
d	energy consumption, J
E	energy efficiency ratio
EER	average energy consumption of precooling
E_{kg}	1 kg of litchi, kJ kg^{-1}
E_{tal}	power consumption of charging and precooling, J
	heat transfer coefficient, W m^{-2} K^{-1}
h	length, m
l	weight, kg
m	number of precooling batches of litchi
n	theoretical energy consumption, W
N_0	heat load, W
P	refrigerating capacity of refrigeration
P_0	system, W
	heat load per unit area, W m^{-2}
q	refrigeration capacity per unit mass, kJ kg^{-1}
q_0	
q_l	density of heat flow rate, W m^{-2}
q_m	mass flow, kg s^{-1}
q_V	refrigeration capacity per unit volume, kJ m^{-3}
Q	
Q_{max}	quantity of heat, J
Q_{chr}	the maximum TES capacity of TES tank, J
r	TES capacity of charging, J
R	radius, m
t	heat conduction resistance, m^2 K W^{-1}
T	time, s or h
TES	temperature, °C
u	thermal energy storage, J
v_{in}	precooling rate, kg h^{-1}
V_R	inspiratory specific volume, m^3 kg^{-1}
V_{th}	volume flow rate, m^3 s^{-1}
w_0	theoretical gas transfer volume, m^3
ΔT	unit theoretical work, kJ kg^{-1}
	temperature difference, °C

Greek symbols

Subscripts

amb	ambient
chr	charging
coi	evaporation coil
com	comprehensive
con	condenser
ctp	the end of charging to the end of precooling
cwp	circulating water pipe
eff	effective TES
eli	energy lost through insulation
eva	evaporator
itw	initial temperature of water
itl	initial temperature of litchi
iw	ice and water
ilt	insulation layer of TES tank
ils	insulation layer of spray precooling box
ilc	insulation layer of circulating water pipe
isc	inner surface of coil
iic	inner surface of insulation layer of circulating water pipe
lit	litchi
load	load of litchi precooling
lod	cooling loss rate caused by opening the door
oic	outer surface of insulation layer of circulating water pipe
osc	outer surface of coil
osi	outer surface of ice
otp	operation of water pump
siw	contact surface between insulation layer and water
spr	spray precooling
spb	spray precooling box
src	contact surface between refrigerant and coil
spa	contact surface between spray precooling box and air
sta	contact surface between TES tank and air
tal	total
thb	thermal bridge
tst	TES tank
ttl	
ttw	

Preprints (www.preprints.org) | NOT PEER-REVIEWED | Posted: 13 June 2023 doi:10.20944/preprints202306.0866.v1

		wat	termination temperature of litchi
α	power coefficient of water pump	*wpp*	precooling
β	volumetric efficiency of compressor	*wpw*	termination precooling temperature of
λ	thermal conductivity, W m^{-1} K^{-1}		water
δ	thickness, m		water
ϱ	density, kg m^{-3}		water pump power
			water pump works on water

2.1. Mathematical model of TES system

During the charging process, the thermal energy is stored in cold water and ice as sensible and latent heat. Cold water storage only contains sensible heat, while ice storage contains both latent heat of ice and sensible heat of cold water. Therefore, latent heat has significant advantages over sensible heat and is the preferred method for energy storage.

In the case of litchi, a precooling system that handles 1000 kg can meet the demand of most small and medium-sized orchards. The suitable storage temperature of litchi is about 5 °C, and it is appropriate to reach 8 °C after precooling. The pulp temperature of litchi is about 29 °C when picked. According to the principle of conservation of energy, the energy absorbed by litchi fruits precooling is calculated as[25]:

$$Q_{lit} = m_{lit} c_{lit} (T_{ttl} - T_{itl}) \tag{1}$$

The TES tank also contains the TES capacity that cannot be used in the precooling process, being the water temperature drops from the initial charging temperature to the termination precooling temperature. There is a significant thermal energy leakage during the refrigeration and storage phases. During precooling, the loss of cooling capacity caused by the water pump working on the water, opening the precooling box and changing the precooling litchi, the connection between the inlet and outlet of the box, and the heat bridge at the edge of the box need to be taken into account in the TES capacity. Therefore, the TES capacity of charging should be improved as follows[26]:

$$Q_{chr} = Q_{lit} + m_{wat} c_{wat} (T_{itw} - T_{ttw}) + P_{eli} t_{ctp} + P_{wpw} t_{otp} + P_{lod} t_{otp} + P_{thb} t_{ctp} \tag{2}$$

$$\frac{dP_{eli}}{dt} = (A_{tst} h_{tst} + A_{spb} h_{spb} + A_{cwp} h_{cwp}) \frac{d(T_{amb} - T_{wat})}{dt} \tag{3}$$

$$\frac{1}{h_{tst}} = \frac{1}{h_{siw}} + \frac{\delta_{ilt}}{\lambda_{ilt}} + \frac{1}{h_{sta}} \tag{4}$$

$$\frac{1}{h_{spb}} = \frac{1}{h_{siw}} + \frac{\delta_{ils}}{\lambda_{ils}} + \frac{1}{h_{spa}} \tag{5}$$

$$\frac{1}{h_{cwp}} = \frac{ln\left(\frac{r_{oic}}{r_{iic}}\right)}{2\pi\lambda_{ilc}} + \frac{1}{h_{spa}} \tag{6}$$

$$P_{wpw} = \alpha P_{wpp} \tag{7}$$

The temperature of ice water mixture is 0 °C after charging, the total TES capacity comprises the sensible heat of water and latent heat of water freezing. Direct evaporation is used for TES and external-melt is used to release thermal energy. Ice is formed directly around the evaporation coil as a regular cylinder. The amount of ice store in TES tank at the end of charging can be estimated using the following equation[27]:

$$m_{ice} C_{ice} = Q_{chr} - m_{wat} c_{wat} T_{itw} \tag{8}$$

$$m_{ice} \rho_{ice} = \pi l_{coi} (r_{ice}^2 - r_{coi}^2) \tag{9}$$

Preprints (www.preprints.org) | NOT PEER-REVIEWED | Posted: 13 June 2023 doi:10.20944/preprints202306.0866.v1

2.2. Thermal resistance of ice-on-coil

Ice-on-coil is a simple and effective TES method with good discharge characteristics. Direct evaporative TES refrigeration system has simple structure and good applicability to small equipment. The structure diagram of evaporation coil icing of the cold storage tank is shown in Figure 2. The coil is horizontal, and the icing state in the TES tank is represented by the evaporation coil per unit length.

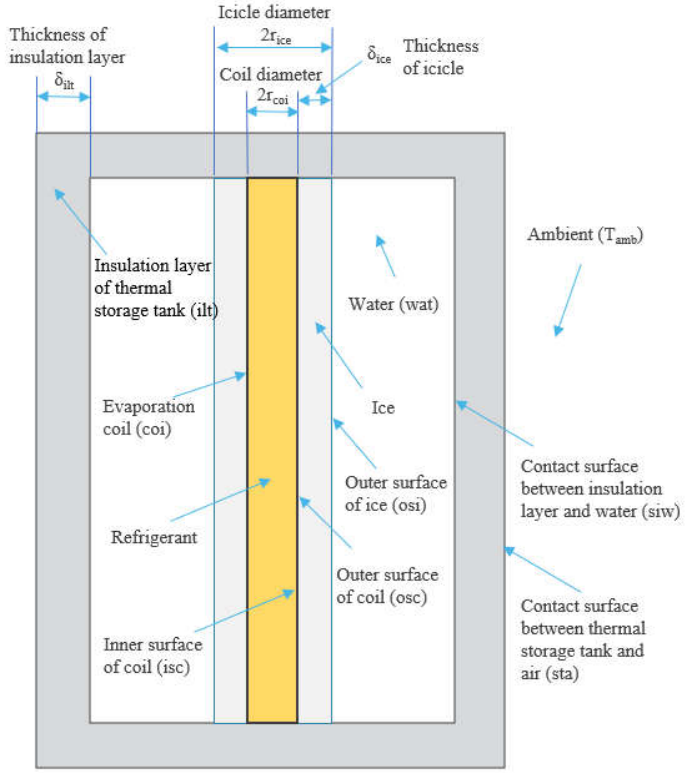

Figure 2. Structure diagram of evaporation coil icing

During the charging process, the refrigerant absorbs heat by evaporation and cools the water outside the coil. Both the thermal resistance between coil and water changes and the heat flow of coil section will change with the increase of ice thickness. According to the fundamental law of heat transfer, the heat flux of the evaporating coil can be expressed using the following equation[28]:

$$q_l = (T_{osi} - T_{eva})h_{com} = \frac{T_{osi} - T_{eva}}{R_{com}} = \frac{T_{osi} - T_{eva}}{R_{src} + R_{coi} + R_{ice} + R_{osi}} \tag{10}$$

The refrigeration system uses R22 refrigerant[29]. The boiling thermal resistance of refrigerant in the coil per unit length can be expressed as[30]:

$$R_{src} = \frac{1}{2\pi r_{isc} h_{isc}} \tag{11}$$

The heat conduction resistance of the evaporated coil per unit length can be expressed as[30],

$$R_{coi} = \frac{1}{2\pi\lambda_{coi}} ln\left(\frac{r_{coi}}{r_{isc}}\right) \tag{12}$$

The heat conduction resistance of ice layer per unit length can be expressed as[30],

$$R_{ice} = \frac{1}{2\pi\lambda_{ice}} ln\left(\frac{r_{osi}}{r_{coi}}\right) \tag{13}$$

The thermal resistance of heat convection between ice and water per unit length can be expressed as[30],

Preprints (www.preprints.org) | NOT PEER-REVIEWED | Posted: 13 June 2023 doi:10.20944/preprints202306.0866.v1

$$R_{osi} = \frac{1}{2\pi r_{osi} h_{osi}} \tag{14}$$

One-dimensional steady-state heat conduction analysis is used to solve the heat transfer process in the cylinder at any time instant. From equation 11-12, it can be seen that increasing the coil radius can reduce the refrigerant evaporation thermal resistance and coil thermal resistance under constant coil thickness. It can be observed from equations 13-14 that R_{ice} increases and R_{siw} decreases with increase ice thickness when the coil radius remains unchanged.

2.3. Mathematical model of refrigeration system

Choosing the matching refrigeration system is important for meeting the TES demand and improving the efficiency of refrigeration. The working characteristics of a refrigeration compressor mainly involve the compressor's refrigerating capacity and the power consumed. The theoretical gas transmission of the compressor is fixed based on the compressor and the refrigeration cycle. The refrigerating capacity and energy consumption are related to the unit refrigerating capacity, unit theoretical work, and compressor's inspiratory capacity of the refrigeration cycle.

According to the thermodynamics of the refrigeration cycle[31], the refrigerating capacity and energy consumption of the refrigeration system are theoretically related as follows,

$$Q_{chr} = P_0 dt - P_{eli} dt - P_{thb} dt \tag{15}$$

$$P_0 = V_R q_V = \beta V_{th} \frac{q_0}{v_{in}} \tag{16}$$

$$N_0 = q_m w_0 = w_0 \frac{V_R}{v_{in}} = \beta V_{th} \cdot \frac{w_0}{v_{in}} \tag{17}$$

The condenser adopts air-cooled forced convection, making it lightweight, small, environmentally friendly, simple, and convenient. According to the fundamental equation of heat transfer[31], the heat transfer area of a condenser is obtained as,

$$A_{con} = \frac{P_{con}}{h_{con} \Delta T_{con}} = \frac{P_0}{q_{con}} \tag{18}$$

Direct evaporative coils are used for ice making in the hydrocooler. The convective heat exchange occurs between the coil and water before freezing, while the exchange is between the coil and ice after freezing. The outer surface area of the coil is taken as the heat transfer area. According to the fundamental equation of heat transfer[31], the heat transfer area of the evaporator is given by,

$$A_{eva} = \frac{P_{eva}}{h_{eva} \Delta T_{eva}} = \frac{P_0}{q_{eva}} \tag{19}$$

$$l_{coi} = \frac{A_{eva}}{2\pi r_{coi}} \tag{20}$$

The values of equations' parameters are summarised in Tab.1. The structural parameters and precooling conditions of the device were assumed, the thermophysical parameters and refrigeration parameters were determined by references, and the environmental and litchi parameters were determined by measurement.

Table 1. Values of equation parameters.

Parameters	Property	Values
A_{cwp}	Area of contact surface between circulating water pipe and air	1.1 m² (Calculated)
A_{spb}	Area of contact surface between spray precooling box and air	4 m² (Assumed)
A_{tst}	Area of contact surface between thermal storage tank and air	10 m² (Assumed)
c_{lit}	Specific heat of litchi	3.704×10^3 J kg^{-1} K^{-1}[32]

Preprints (www.preprints.org) | NOT PEER-REVIEWED | Posted: 13 June 2023 doi:10.20944/preprints202306.0866.v1

c_{wat}	Specific heat of water	4.2×10^3 J kg^{-1} K^{-1}[33]
C_{ice}	Latent heat of water freezing	3.35×10^5 J kg^{-1}[33]
h_{isc}	Boiling coefficient of heat transfer on the refrigerant in the coil	4000 W m^{-2} K^{-1}[33]
h_{osi}	Convective heat transfer coefficient between ice and water	400 W m^{-2} K^{-1}[33]
h_{siw}	Convection heat transfer coefficient of water and thermal storage tank	100 W m^{-2} K^{-1}[33]
h_{spa}	Convection heat transfer coefficient of spray precooling box and air	20 W m^{-2} K^{-1} (Measured)
h_{sta}	Convection heat transfer coefficient of thermal storage tank and air	6 W m^{-2} K^{-1} (Measured)
m_{lit}	The mass of litchi precooling	1000 kg (Assumed)
m_{wat}	The mass of water in thermal storage tank	1200 kg (Assumed)
P_{lod}	Cooling loss rate caused by opening the door	300 W (Assumed)
P_{thb}	Power of heat bridge heat transfer	200 W (Assumed)
P_{wpp}	Water pump power in precooling	280 W (Calculated)
q_{con}	Heat load per unit area of the condenser	260 W m^{-2}[31]
q_{eva}	Heat load per unit area of the evaporator	3500 W m^{-2}[31]
r_{coi}	Radius of evaporation coil	0.008 m (Assumed)
r_{iic}	Radius of circulating water pipe	0.032 m (Assumed)
r_{isc}	Inner radius of evaporation coil	0.007 m (Follow determination)
r_{oic}	Radius of circulating water pipe insulation layer	0.072 m (Follow determination)
t_{chr}	Charging time of thermal storage	12 h (Assumed)
t_{ctp}	Time from the end of charging to the end of precooling	12 h (Assumed)
t_{otp}	Operation time of water pump	8 h (Assumed)
T_{amb}	The ambient temperature	30 °C (Measured)
T_{ilt}	The initial temperature of litchi precooling	29 °C (Measured)
T_{itw}	The initial temperature of water	31 °C (Measured)
T_{osi}	Outer surface temperature of ice	0 °C (Assumed)
T_{ttl}	The termination temperature of litchi precooling	8 °C (Assumed)
T_{ttw}	The termination precooling temperature of water	7 °C (Assumed)
T_{wat}	The water temperature of thermal storage tank	15 °C charging (Assumed) 3 °C after charging (Assumed)
α	The power coefficient of water pump	0.57 (Measured)
δ_{ils}	Insulation layer thickness of spray hydrocooling box	0.01 m (Assumed)
δ_{ilt}	Insulation layer thickness of thermal storage tank	0.05 m (Assumed)
λ_{coi}	Coil's thermal conductivity	377 W m^{-1} K^{-1} [33]
λ_{ice}	Ice layer's thermal conductivity	2.22 W m^{-1} K^{-1} [33]
λ_{ilc}	Insulation layer thermal conductivity	0.038 W m^{-1} K^{-1} [33]
λ_{ils}	Insulation layer thermal conductivity	0.038 W m^{-1} K^{-1} [33]
λ_{ilt}	Insulation layer thermal conductivity	0.038 W m^{-1} K^{-1}[33]
ρ_{ice}	Density of ice	920 kg m^{-3} [33]

2.4. Solution of mathematical model

The weight of litchi precooling for the hydrocooler is dependent on the current situation of the orchard. According to equation 1 and physical parameters of litchi, 1000 kg litchi precooling required

Preprints (www.preprints.org) | NOT PEER-REVIEWED | Posted: 13 June 2023 doi:10.20944/preprints202306.0866.v1

thermal energy capacity Q_{lit} of 8.1×10^7 J. Solving equations 2-7, the TES capacity Q_{chr} of the TES tank was 2.4 × 10^8 J, and the ice volume reached 256 kg.

The relationship between ice thickness and heat transfer coefficient can be obtained according to equations 10-14, as shown in Figure 3. The thermal resistance increases while the heat transfer coefficient decreases with the increase of ice thickness. The total heat transfer coefficient is 17.875 W m^{-2} K^{-1}, and the total thermal resistance is 0.056 m^2 K W^{-1} when ice is not formed. The heat transfer coefficient decreases rapidly with ice thickness when the ice thickness is less than 40 mm. The heat transfer coefficient decreases significantly with ice thickness when the thickness is greater than 40 mm. The total thermal resistance is 0.143 m^2 K W^{-1}, and the heat transfer coefficient is 6.995 W m^{-2} K^{-1}, which is 60.9% lower than that without ice when the ice thickness is 40 mm. Once the ice thickness exceeds 120 mm, the heat transfer coefficient reduces slowly.

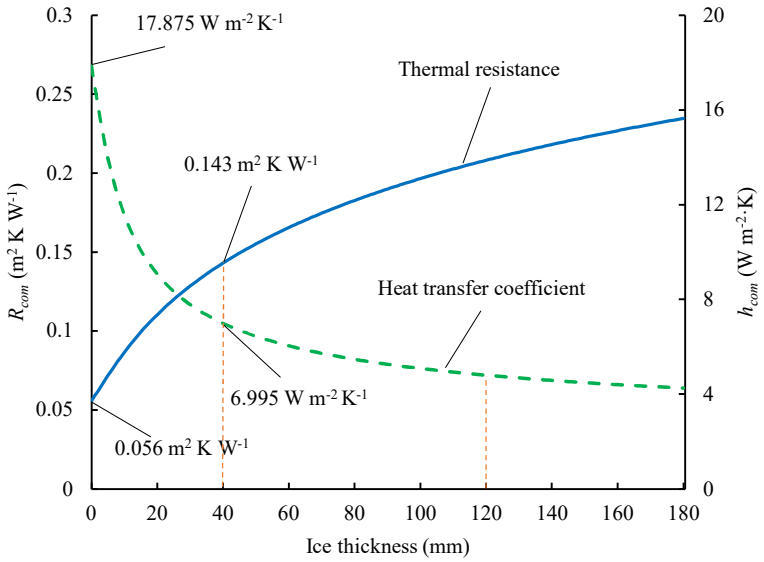

Figure 3. The variation of the total thermal resistance and heat transfer coefficient with the ice thickness.

Given the thermal resistance analysis of the ice-on-coil, the best ice thickness was considered to be 40 mm. According to equation 9, the evaporation coil length was 39.5 m. If using a single coil with 39.5 m, excessive coil length would increase the superheat, reduce the return air pressure and cause the suction gas of the compressor to overheat and produce low refrigerant efficiency of refrigeration system. According to equation 15, the refrigerating capacity of the compression should reach 5900 W in order to meet the TES demand in 12 h. Therefore, the cooling was divided into two refrigeration units, the refrigerating capacity of each refrigeration system should reach 2950 W. From equation 18, the condensation heat transfer area of the condenser is calculated to be greater than 11.3 m^2 for a single refrigeration unit. Solving for equation 19 determines that the evaporation heat transfer area of the evaporator should be greater than 0.84 m^2 for a single refrigeration unit. The length of the evaporation coil was 19.75 m of a single refrigeration unit, so the outer surface area of the evaporation coil of a single refrigeration unit was 1 m^2, which met the requirements of evaporation heat transfer area. The solutions of equations and determination of ice thickness are summarised in Tab. 2.

Preprints (www.preprints.org) | NOT PEER-REVIEWED | Posted: 13 June 2023 doi:10.20944/preprints202306.0866.v1

Table 2. Solutions of equations and ice thickness determination.

Parameters	Property	Values	The reference equations
Q_{lit}	Thermal energy absorbed by litchi precooling	8.1×10^7 J	Equation (1)
Q_{chr}	TES capacity of charging	2.4×10^8 J	Equation (2)-(7)
m_{ice}	Ice storage capacity of charging	256 kg	Equation (8)
δ_{ice}	Thickness of icicle	0.04 m	Figure 3 and Equation (10)-(14)
l_{coi}	Length of evaporation coil	39.6 m	Equation (9)
P_0	Refrigerating capacity of compressor	5900 W	Equation (15)-(17)
A_{con}	Heat transfer area of condenser	22.6 m^2	Equation (18)
A_{eva}	Heat transfer area of evaporator	2 m^2	Equation (19)-(20)

3. Design and fabrication of hydrocooler

3.1. Overall structure

The hydrocooler combines the functions of refrigeration, storage, and precooling to make the device portable. The TES system and spray hydrocooling system were designed to realise the required thermal energy transfer. The hydrocooler based on the TES technology was designed by analysing the TES capacity, heat transfer characteristics, and refrigeration system configuration. The hydrocooler was composed mainly of the refrigeration unit, thermal storage tank, spray precooling box, circulating water pipe, water pump, and the base plate shown in Figure 4.

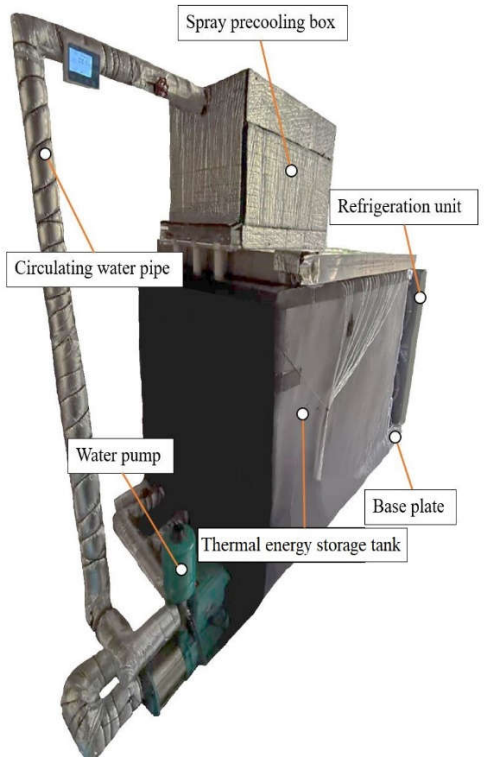

Figure. 4. Photograph of the spray hydrocooler.

The refrigeration capacity of one QXL-30E compressor was 3180 W when the evaporation temperature was –10 °C. Hence, the refrigeration capacity of two systems was 6360 W that met the calculation requirements in Section 2. Two air-cooled condensers from SIMCO (SIMCO, small 3-HP, China) with 18 m^2 heat transfer area each were used. According to Section 2, the heat transfer area, A_{eva}, of the evaporator exceed 1 m^2, and the coil length, L, was not less than 39.6 m. Here the length of evaporation coil was 43.4 m of two refrigeration units. The circulating water pipe with a diameter

Preprints (www.preprints.org) | NOT PEER-REVIEWED | Posted: 13 June 2023 doi:10.20944/preprints202306.0866.v1

of 32 mm and Weller sd-750 variable frequency water pump were selected, and the maximum flow reached 200 L min^{-1}. The spray precooling method was adopted to realize the rapid precooling of the fruit. The sprinkler was selected as the spray structure, which had high uniformity and pressure regulation characteristics. The size of a single sprinkler was 0.25×0.25×0.006 m^3. The diameter of nozzle was 1.5mm, which was made of silica gel. The spray structure was made up of 6 sprinklers. The size of spray precooling tank was 0.75×0.52×0.45 m^3, two precooling baskets could be placed at the same time. The size of the cold storage tank was 1.7×0.85×1 m^3, and the maximum water storage was 1.2 m^3. The parameters of the spray hydrocooler are shown in Tab. 3.

Table 3. Selection of spray hydrocooler components.

Component	Size or model	Material or company	Values
Compressor	QXL-30E	Zhejiang Boyang	3180 W(-10 °C)
Condenser	Small 3-HP	SIMCO	18 m^2×2
Evaporation coil	0.016 m diameter	Copper	43.4 m
Circulating water pipe	0.032 m diameter	PVC	5 m
Thermal energy storage tank	1.7 × 0.85 × 1 m^3	Stainless-steel	1.4 m^3
Spray precooling box	0.75 × 0.52 × 0.45 m^3	Acrylic	0.18 m^3
Nozzle	0.0015 m diameter	Silica gel	Variable size
Sprinkle	0.25 × 0.25 × 0.006 m^3	Stainless-steel	3-10 L min^{-1}×6
Precooling basket	0.35×0.48×0.16 m^3	Plastic	200 g
Water pump	SD-750	Weller	Frequency conversion

3.2. Structure of TES system

The structure of TES tank and refrigeration system are shown in Figure 5. The evaporation coil layout is shown in Figure 5b. The coils' centre was kept 120 mm apart horizontally and 135 mm apart vertically to avoid overlapping of ice. The coils in the first, third, and fifth layers were connected to the first compressor, while the coils of the second, fourth, and sixth layers were connected to the second compressor. During the charging process, the refrigerant flows into the first and second layers' coils and flows out through the coils in the fifth and sixth layers respectively.

Preprints (www.preprints.org) | NOT PEER-REVIEWED | Posted: 13 June 2023 doi:10.20944/preprints202306.0866.v1

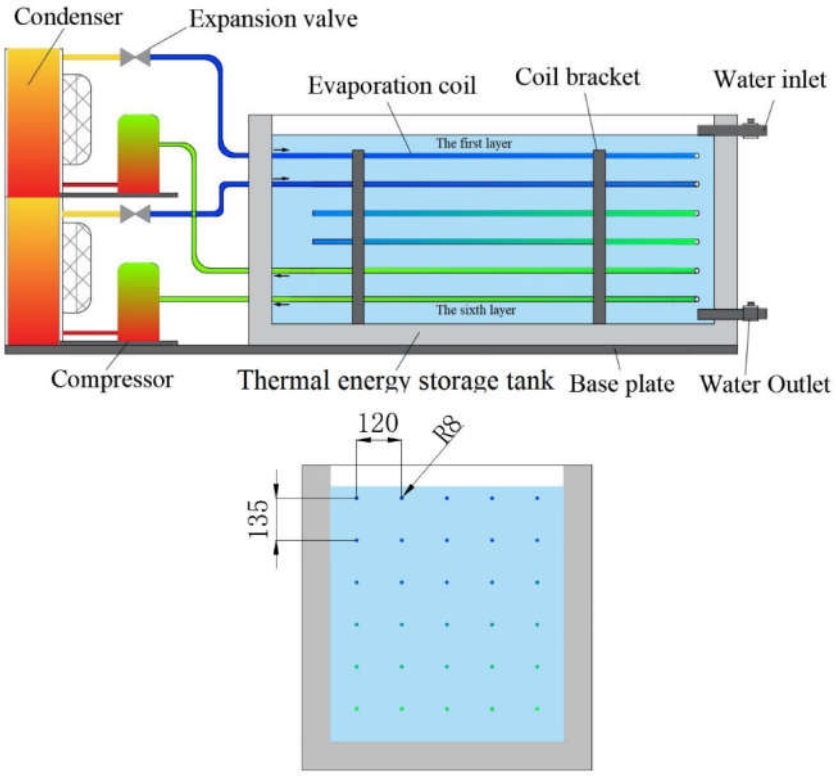

Figure 5. Structure diagram of TES tank and refrigeration system.

3.3. Structure of spray hydrocooling system

The precooling device was designed with a precooling capacity of 1000 kg litchi per day and a precooling time of 8 h. If 6 batches were precooled per hour, the precooling capacity of each batch was 21 kg. The size of packing basket selected was 0.35×0.48×0.16 m^3, and each basket could hold 11.5 kg of litchi. Figure 6 shows the schematic diagram and photograph of the spray precooling box. Sprinkler were mounted at the top and a perforated plate used at the bottom of spray hydrocooling box. The outside of the box is covered with 1cm thick insulation cotton. Six square stainless-steel sprinklers had nozzles made of silica gel. The nozzles are 1.5 mm diameter under zero-pressure conditions and enlarge with water pressure. The spray flow rate is controlled by the variable frequency water pump. Litchi packed in perforated baskets are kept in the spray precooling box for precooling. The cold water sprayed over the litchi initiates rapid heat exchange. The water then flows through the perforated bottom plate and enters the TES tank.

Preprints (www.preprints.org) | NOT PEER-REVIEWED | Posted: 13 June 2023 doi:10.20944/preprints202306.0866.v1

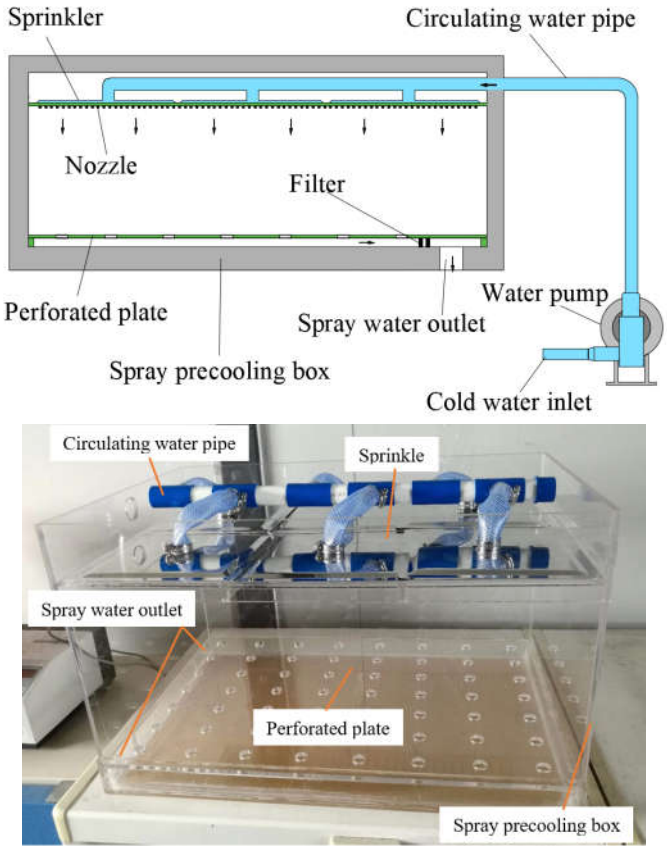

Figure 6. Schematic diagram and photograph of spray precooling box and cold-water circulation system.

4. Charging test and litchi spray precooling tests

4.1. Experimental setup

The experimental setup was shown in Figure 4, the TES tank was covered with 50 mm thick insulation cotton, the spray hydrocooling box was covered with 10 mm thick insulation cotton and the circulating water pipe was covered with 20mm thick insulation cotton to prevent energy leakage. The experiment was carried out using a VX810 paperless recorder (Hangzhou Pangu Automation System Co., Ltd.) for data recording at 1 s frequency. PT100 temperature sensor (±0.1 °C) for temperature monitoring, and KAA-T4 AC transmitter (0–30 A, ±0.2%, Zhuhai Xinghui Electronic Technology Co., Ltd.) for measuring water pump and compressor power consumption. As shown in Figure 7, 27 PT100 temperature sensors were arranged in a 3×3×3 array. One (1) charging test and eleven (11) litchi spray precooling tests were conducted (Table 4).

4.2. Charging test

During the charging test, the TES tank contained 1200kg water with an initial temperature of 31 °C. The TES tank was charged for 12 h. As shown in Figure 7, three ice thickness measuring points, a, b, and c in the first, third, and fifth layers of coil respectively, were used to manually estimate ice mass manually through observing the scale. The ice thickness was manually measured every 30 minutes through the method of observing the scale. The scales were fixed on the coil horizontally with the circle center of the coil. When water outside of the coil was frozen, the contact position between the outer surface of the ice layer and the scale was considered the ice thickness (d_{ice}). The aim was to analyse the TES capacity and economy of hydrocooler with increase charging time.

4.3. Litchi spray precooling tests

Conditions of spray hydrocooling tests are shown in Tab. 4, there are 3 test conditions were listed, which were charging time, litchi load and spray flow rate. This design is a hub and spoke type

Preprints (www.preprints.org) | NOT PEER-REVIEWED | Posted: 13 June 2023 doi:10.20944/preprints202306.0866.v1

experimental design where the test 2 (4h, 23 kg, 30 L min^{-1}) was in the central location and then explored the ranges of the three parameters in both directions. The spray precooling test was to study different test conditions and identify the best operating parameters of the spray hydrocooling box. There are 5 litchis were selected from the middle layer of litchi basket for monitoring pump temperatures, and PT100 temperature sensors were inserted in litchis pulp respectively. The litchi was taken out when the pulp temperature dropped to 8 °C, and replace with the litchi to be precooled. This was repeated until the water temperature of the TES tank reached 7 °C, ending precooling test.

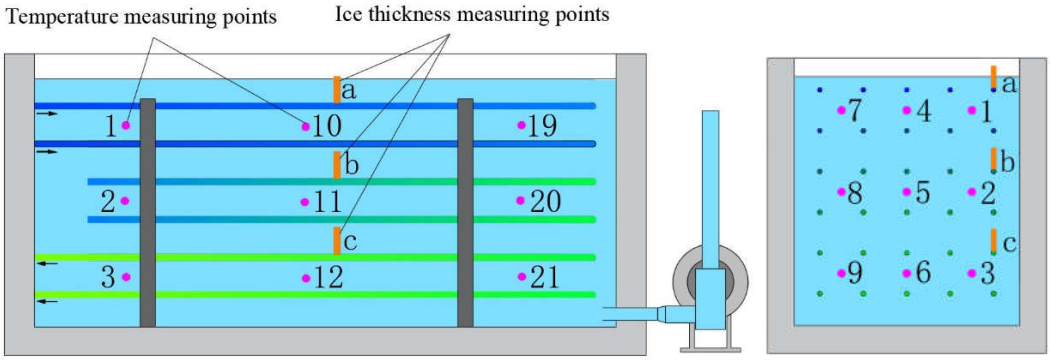

Figure 7. Temperature measuring and ice thickness measuring points of the spray hydrocooler.

Table 4. Conditions of charging and spray hydrocooling tests.

Test	Charging time (h)	Litchi load (kg)	Spray flow rate (L min^{-1})	Water storage capacity of TES tank (kg)
1	12	--	--	1200
2	4	23	30	400
3	3	23	30	400
4	5	23	30	400
5	6	23	30	400
6	5	8	30	400
7	5	13	30	400
8	5	18	30	400
9	5	28	30	400
10	5	23	20	400
11	5	23	40	400
12	5	23	50	400

* Test 1 was charging test, tests 2-12 were litchi spray hydrocooling test, test 2 = central comparison point, tests 3-5 = charging time, tests 6-8 = litchi load and tests 9-11= spray flow rate.

4.4. Evaluation of spray hydrocooler performance

The water temperature (T_{wat}) was measured at three different layers (upper, middle and the lower) in the TES tank with 9 temperature sensors in each layer. In the charging process, the water temperature of each layer was considered the average value. During litchi precooling, the water temperature was represented by the mean value of these 27 temperature sensors.

Ice thickness, δ_{ice}, as shown in Figure 2, it was the average value of the ice thickness.

The TES capacity (Q_{chr}) indicated the sensible heat released by the water cooling and latent heat released by the water freezing. It could be expressed as:

$$Q_{chr} = m_{wat}c_{wat}(t_{itw} - t_{wat}) + m_{ice}(c_{wat}t_{wat} + C_{ice}) \quad (21)$$

Preprints (www.preprints.org) | NOT PEER-REVIEWED | Posted: 13 June 2023 doi:10.20944/preprints202306.0866.v1

The effect TES capacity (Q_{eff}) refers to the thermal energy storage that can be used by litchi precooling. It was the part that uses the TES capacity to subtract the part that cannot be used, that was the part where the water temperature of the TES tank decreases from the initial temperature to the end of precooling temperature. It can be expressed as[44]:

$$Q_{eff} = Q_{chr-}m_{wat}c_{wat}(t_{itw} - t_{ttw}) = m_{wat}c_{wat}(t_{ttw} - t_{wat}) + m_{ice}(c_{wat}t_{wat} + C_{ice}) \quad (22)$$

$$m_{ice} = \rho_{ice}\pi l_{coi}\left[\left(\frac{\sum(\delta_{ice} + r_{coi})}{3}\right)^2 - {r_{coi}}^2\right] \quad (23)$$

The total power consumption (E_{tal}) including water pump power consumption in the spray precooling test and compressor power consumption in charging process can be expressed as:

$$E_{tal} = E_{spr} + E_{chr} \quad (24)$$

EER, the energy efficiency ratio is the ratio of TES capacity to power consumption. In order to obtain the real-time energy efficiency change and average energy efficiency change of the charging process, a 30 min energy efficiency ratio and average energy efficiency ratio are used. The 30 min energy efficiency ratio is the ratio of TES capacity and the energy consumption in 30 minutes, the average energy efficiency ratio is the ratio of TES capacity and the energy consumption since the beginning of charging. All expressed as[34]:

$$EER = \frac{Q_{chr}}{E_{chr}} \quad (25)$$

Precooling capacity (m_{spr}) refers to the precooling capacity refer to the total amount of litchi precooled until finishing precooling in one test.

Precooling time (t_{spr}), the precooling time refers to the time from the beginning of precooling to the finish precooling in one test when the water reaches 7 °C.

Precooling rate (u_{spr}), ratio of precooling capacity to precooling time in one test.

Average power consumption (E_{kg}), is the power consumption per kilogram litchi precooled. It is the most intuitive method to evaluate the cost of litchi precooling and an important index to evaluate the economy of precooling equipment. The average power consumption is given by:

$$E_{kg} = \frac{E_{tal}}{m_{spr}} \quad (26)$$

5. Results and discussions

5.1. Experiment Ⅰ: Charging of TES tank

5.1.1. Variation of water temperature and ice thickness

The variation of water temperature and ice thickness are shown in Figure 8. The water temperature decreased rapidly with charging time during the first 6 h, but the decrease became more gradual when the water temperature was lower than 5 °C. Before 6 h, the upper layer's water temperature was higher than the lower and middle layers. From 0-6 h, the lower layer's temperature was higher than the upper and middle layers. After 9 h, the water temperature remained almost unchanged and was in the range of 1.4 °C and 2 °C. The water density increases with the decrease of temperature when the water temperature is higher than 4 °C. The water density drops as the temperature decreases when the water temperature is lower than 4 °C. Hence, the sinking of colder water leads to the upper layer's water temperature higher than the lower and middle layers when water is higher than 4 °C. On the contrary, the floating of colder water leads to the lower layer's water temperature was higher than the upper and middle layers when the water temperature is lower than 4 °C[35].

Preprints (www.preprints.org) | NOT PEER-REVIEWED | Posted: 13 June 2023 doi:10.20944/preprints202306.0866.v1

It can be seen from figure 8, the water around coils begins to freeze at 3.5 h. Initially, the ice thickness of the lower layer was more than the upper and middle layers. After 7 h of charging, the lower layer's ice thickness was less than the upper and middle layers. The temperature of the lower layer was more than the upper and middle layers after 6 h, which resulted in reduced ice thickness in the lower layer after 7 h of charging. The ice thickness of upper, middle, and lower layers after 12 h of charging was 42 mm, 42 mm, and 39 mm, respectively, the average ice thickness was 41 mm which is close to the designed thickness of 40 mm. The mass of ice from the two refrigeration units was 143.3 kg and 141.3 kg, respectively, after 12 h of charging. The total ice storage capacity was 284.6 kg, which meets the design requirements of m_{ice} less than 272.5 kg.

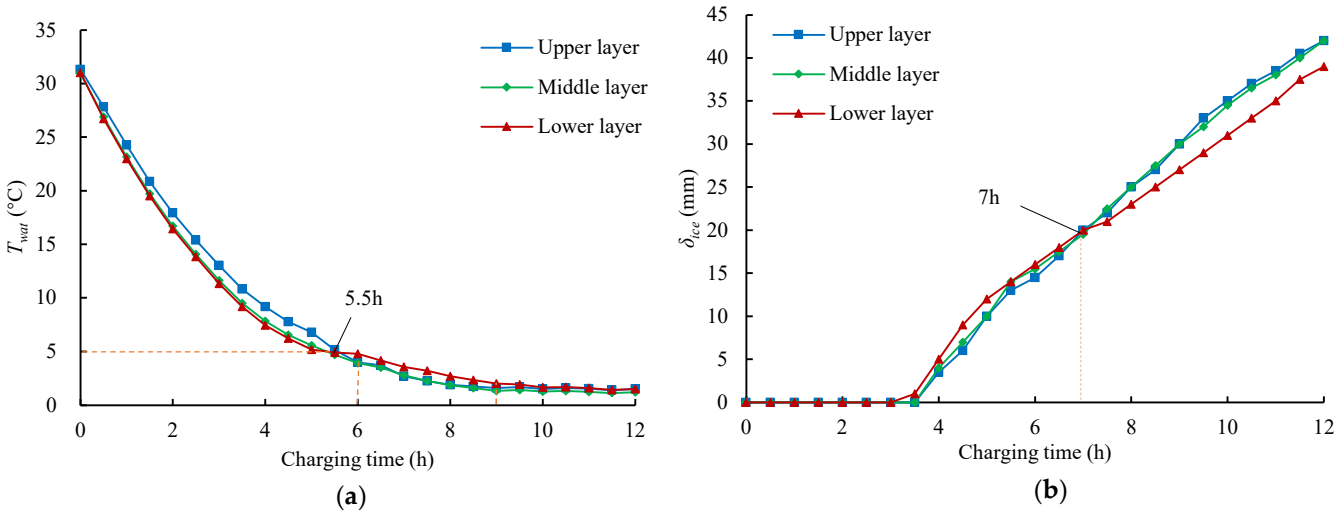

Figure 8. Plots showing variation of (**a**) water temperature and (**b**) ice thickness of different layers with charging.

5.1.2. Variation of TES capacity and EER

Figure 9 shows the changes of TES capacity and effective TES capacity with charging time. It can be seen from the figure that the TES capacity continued to increase, and the effective TES capacity was 0 in the first 4 h. After 4 h of charging, the effective TES capacity began to linear increase. After 12 h charging, the effective TES capacity reached 1.25×10^8 J. The TES capacity was 2.47×10^8 J, which was twice the effective TES capacity. It can be seen from Section 2.4 that the design TES capacity of the device was 2.4×10^8 J, and the test value met the design requirements. The remaining 1/2 TES capacity that cannot be utilized was used to reduce the water temperature from initial state to 7 °C. If the remaining 1/2 TES capacity for reducing the water temperature of the TES tank can be reused, the power consumed by charging will be greatly reduced.

As shown in Figure 10, the 30 min EER in charging was stable and the maximum was 3.56 in one hour. It decreased rapidly after 1.5 h, and reached 1.24 at 6.5 h. Then followed by fluctuation, it reached the minimum value of 1.12 at 12 h. It showed that the efficiency of charging was high at the beginning, then decreased rapidly, and remained stable after 6 h. The fluctuation of EER during the charging process was due to the measurement error of TES capacity. But the fluctuation can't influence the overall trend of EER in charging. However, the average EER was 3.5 at the beginning of the charging process, and gradually decreased after 1 hour, reached the lowest value of 2.0 at 12 h. From Figure 10 we can know, the longer the charging time is, the lower the EER of TES is.

Preprints (www.preprints.org) | NOT PEER-REVIEWED | Posted: 13 June 2023 doi:10.20944/preprints202306.0866.v1

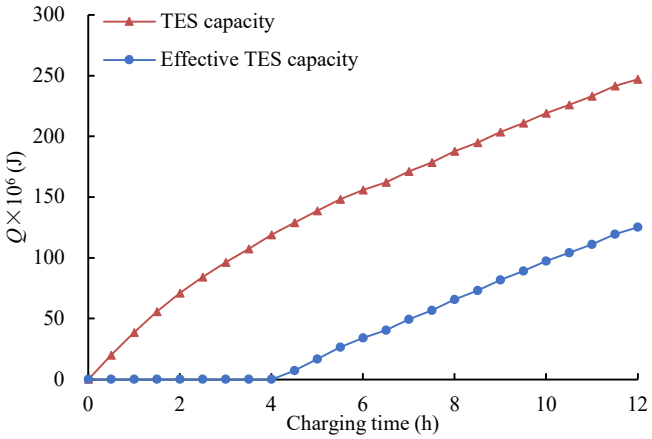

Figure 9. Plots showing variation of TES capacity and effective TES capacity with charging.

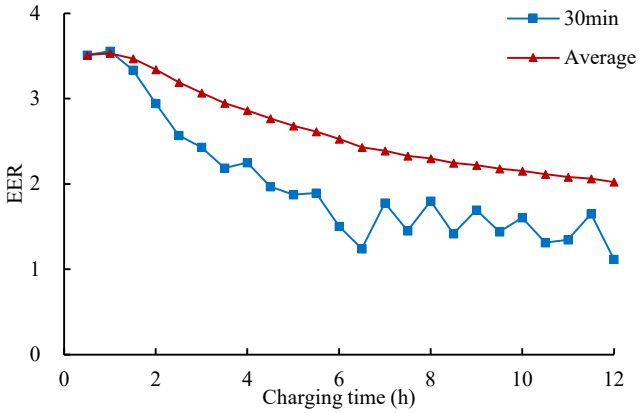

Figure 10. Plots showing variation of energy efficiency ratio of hydrocooler with charging.

5.2. Experiment II: litchi spray hydrocooling performance

5.2.1. The temperature of litchi and water

Figure 11 shows the variation curve of water temperature and litchi temperature during litchi precooling in test 2. It can be seen from the figure that the initial temperature of litchi was about 30 °C, and the end temperature of litchi precooling was 8 °C. There were 9 batches and a total of 207 kg of litchi that were precooled. The precooling water temperatures of 9 batches of litchi were 2.22 °C, 3.14 °C, 3.71 °C, 4.16 °C, 4.5 °C, 4.86 °C, 5.23 °C, 5.84 °C, 6.53 °C, and the precooling times were 6.53 min, 11.27 min, 8.3 min, 10.83 min, 9.53 min, 10.97 min, 10.97 min, 15.4 min and 12.63 min respectively. The average precooling time of a single batch was 11 min, which was 10% higher than the design value. During the precooling process, all the ice had melted when the water temperature reached 7 °C, and the water temperature of the TES tank rised steadily.

Preprints (www.preprints.org) | NOT PEER-REVIEWED | Posted: 13 June 2023 doi:10.20944/preprints202306.0866.v1

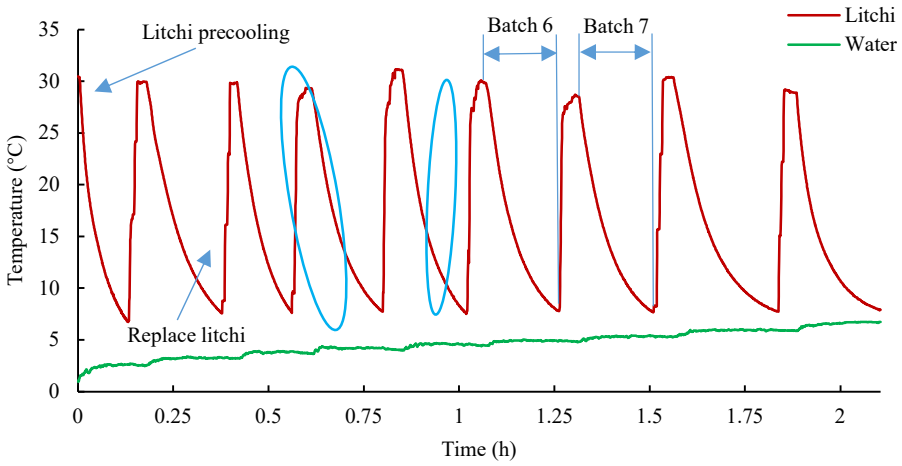

Figure 11. The temperature curve of litchi spray hydrocooling in test 2.

5.2.2. Precooling capacity and precooling rate

Figure 12 shows the litchi spray precooling capacity and precooling rate for litchi at different experimental conditions. Figure 12a shows that the precooling capacity increased simultaneously with charging time while the precooling rate did not change significantly. It was obvious that the precooling rate of 5 and 6 charging tests were faster than that of 3 and 4 h charging tests. The weight of litchi precooled reached 299 kg after 6 h charging with one-third water of TES tank. When the TES tank was full of water, the precooling capacity of litchi would exceed 900 kg. Because the TES capacity increases, the relative thermal energy loss will decrease. Figure 12b shows that the precooling capacity initially increased and then decreased with increase of litchi load. The precooling rate significantly rise until the litchi load was more than 23 kg. The maximum precooling capacity was 207 kg and the maximum precooling rate was 94.1 kg h^{-1} when the litchi load was 23 kg. Figure 12c shows that the precooling capacity at 30 L min^{-1} was higher than other spray flow rate. When the spray flow rate was 50 L min^{-1}, it had a minimum precooling capacity. The precooling rate at 50 L min^{-1} was higher than other spray flow rate, when the spray flow rate was 30 L min^{-1}, it had a minimum precooling rate. The precooling capacity and precooling rate for different spray flow rates had a small difference. Overall, the precooling capacity obviously increased with increase of charging time, and precooling rate went up with the increase in the litchi load when the litchi load was less than 23 kg.

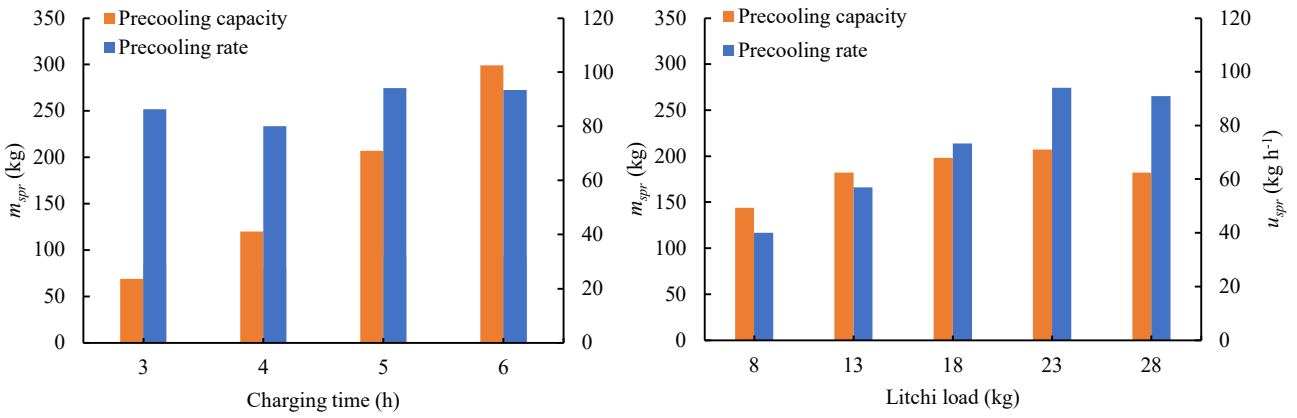

(**a**) (**b**)

Preprints (www.preprints.org) | NOT PEER-REVIEWED | Posted: 13 June 2023 doi:10.20944/preprints202306.0866.v1

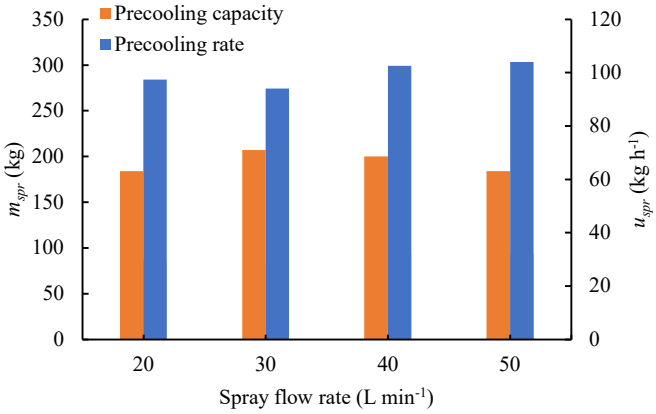

(**c**)

Figure 12. Variation of precooling capacity and precooling rate under different (**a**) charging time, (**b**) litchi load, and (**c**) spray flow rate.

5.2.3. Total power consumption and average power consumption

Figure 13 shows the total power consumption and average power consumption of litchi spray precooling at different experimental conditions. Figure 13a shows that charging and precooling power consumption increases with charging time, and charging power consumption was significantly higher than that of precooling. In contrast, the average power consumption of litchi decreased significantly with increases in charging time. The average power consumption of litchi precooling was 437 kJ kg^{-1}, 349 kJ kg^{-1}, 250 kJ kg^{-1}, and 193 kJ kg^{-1} for charging times of 3 h, 4 h, 5 h, and 6 h, respectively. The average cost can be reduced by increasing the TES capacity within the limits of the hydrocooler capacity. Figure 13b and 13c shows a little power consumption difference during 4 h charging in different tests. There was probably an environmental effect at natural condition. The maximum energy consumption difference in the charging process was 2.52×10^6 J.

From Figure 13b can be seen that the precooling energy consumption significant increase with low litchi load and average energy consumption also significant increase with low litchi load. When the litchi load reaches 8 kg, the maximum average energy consumption is 383 kJ kg^{-1}. The minimum average power consumption is 250 kJ kg^{-1} when the litchi load was 23kg. As seen in Figure 14c, the minimum average power consumption of litchi was at spray flow rate of 30 L min^{-1}, and 40 L min^{-1} spray flow rate was a little higher. The average power consumption of 30 L min^{-1} and 40 L min^{-1} spray flow rate were 243 kJ kg^{-1} and 253 kJ kg^{-1}, respectively. The optimal spray flow rate is 30 L min^{-1} in litchi spray precooling, followed by 40 L min^{-1}.

Preprints (www.preprints.org) | NOT PEER-REVIEWED | Posted: 13 June 2023 doi:10.20944/preprints202306.0866.v1

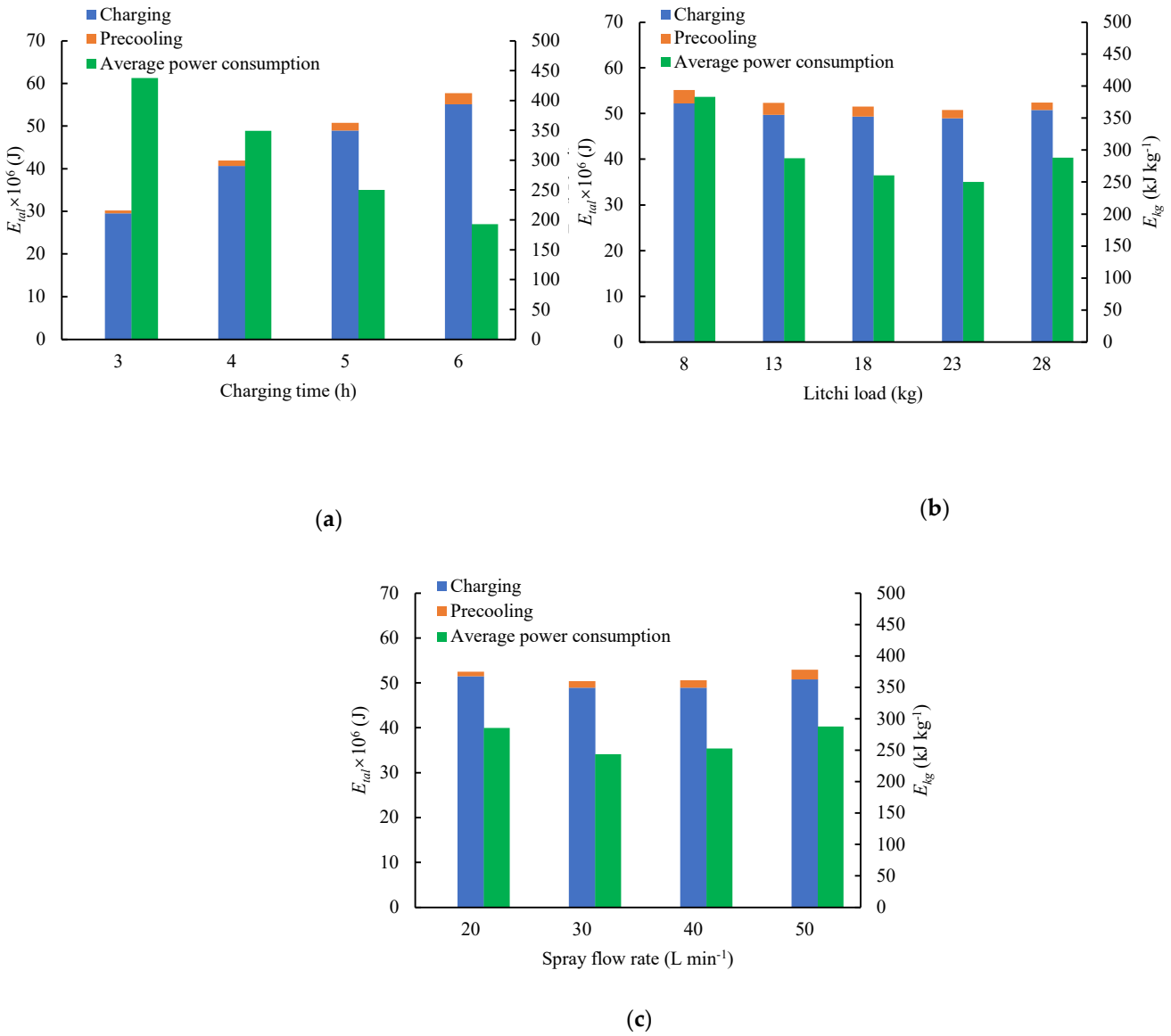

Figure 13. Variation of total power consumption and average power consumption of spray hydrocooler under different (**a**) charging time, (**b**) litchi load, and (**c**) spray flow rate.

6. Conclusions

In this study, a novel spray hydrocooler based on TES was developed, manufactured, and tested.

(1) The capacity of TES, the thermal resistance of ice-on-coil, and the refrigeration system were analysed theoretically. The structure and components of the spray hydrocooler were designed and tested.

(2) Charging test and litchi spray precooling experiments were carried out at different charging times, spray flow rate, and litchi load. The results showed that the spray hydrocooler can achieve the rapid and effective precooling of litchi in the producing regions.

(3) In the charging process, the ice thickness was 41 mm, the ice storage capacity was 284.6 kg, and the TES capacity was 2.47×10^8 J after 12 h charging, which meets the design requirements. Charging time was the most important factor influencing the precooling capacity and average power consumption. Increasing charging time was an effective way to increase the precooling capacity and reduce the average power consumption.

(4) In litchi precooling process, when the litchi load is 23 kg and spray flow rate is 30 L min^{-1}, the spray hydrocooler has the largest precooling capacity and the smallest average power consumption of litchi spray precooling.

The precooler provides a feasible scheme for precooling litchi in small orchards. Simultaneously, the use of valley value electricity price for TES can significantly reduce the operating cost. In the future, improving the energy efficiency of ice-on-coil, the utilisation rate of a thermal storage tank, and the cooling uniformity of litchi can improve the performance of the spray hydrocooler.

Author Contributions: Conceptualization, Hao Huang and Enli Lv; methodology, Hao Huang and Jiaming Guo; validation, Hao Huang; formal analysis, Jiaming Guo; investigation, Hao Huang; resources, Enli Lv; writing—original draft preparation, Hao Huang; writing—review and editing, Jiaming Guo; supervision, Enli Lv and Huazhong Lu; project administration, Hao Huang; project administration, Jiaming Guo; funding acquisition, Enli Lv, Huazhong Lu and Jiaming Guo. All authors have read and agreed to the published version of the manuscript.

Funding: This study was funded by the National Natural Science Foundation of China (Grant No. 31971806), the National industrial technology system of litchi and longan Program of China (Grant No. CARS-32-11) , the Guangdong Provincial Agricultural Technology Innovation and Promotion Project in 2019 (Grant No. 2023KJ101), the Research and Development and Innovation Team of Common Key Technologies for Agricultural-Product Preservation Logistics (Grant No. 2023KJ145), and the Guangdong Province Agricultural scientific research projects and agricultural technology promotion Program (Grant No. 440000210000000086860). These supports are gratefully acknowledged.

Data Availability Statement: The data that support the findings of this study are available from the corresponding author upon reasonable request.

Conflicts of Interest: No conflict of interest exists in the submission of this manuscript.

References

1. Hui L, Huang D, Ma Q, et al. Factors influencing the technology adoption behaviours of litchi farmers in China. Sustainability. 2020, 12(1): 271.
2. Yuan D, Wang G, Fawole O A, et al. Postharvest precooling of fruit and vegetables: A review. Trends in Food Science & Technology. 2020, 100: 278-291.
3. Xin-yu Bai,Zi-meng Yang,Wan-jun Shen, et al. Polyphenol treatment delays the browning of litchi pericarps and promotes the total antioxidant capacity of litchi fruit[J]. Scientia Horticulturae, 2022, 291.
4. Kumari P, Kalyan B, Patel V B, et al. Reducing postharvest pericarp browning and preserving health promoting compounds of litchi fruit by combination treatment of salicylic acid and chitosan. Scientia Horticulturae. 2015, 197: 555-563.
5. Edna Makule,Noel Dimoso,Savvas A. Tassou. Precooling and Cold Storage Methods for Fruits and Vegetables in Sub-Saharan Africa—A Review[J]. Horticulturae, 2022, 8(9).
6. Wang G, Zhang X. Evaluation and optimization of air-based precooling for higher postharvest quality: literature review and interdisciplinary perspective. Food Quality and Safety. 2020, 4(2): 59-68.
7. Zhao H, Sheng L, Tian C, et al. An overview of current status of cold chain in China. International Journal of Refrigeration. 2018, 88: 483-495.
8. Sena E A, Da silva P O, De A S, et al. Postharvest quality of cashew apple after hydrocooling and coold room. Postharvest Biology and Technology. 2019, 155: 65-71.
9. Ilknur A, Nezihe K. Forced-air, vacuum, and hydro precooling of cauliflower (Brassica oleracea L. var. botrytis cv. Freemont): Part II. Determination of quality parameters during storage. Food Science and Technology. 2015, 35(1): 45-50.
10. O'sullivan J L, Ferrua M J, Love R, et al. Forced-air cooling of polylined horticultural produce: Optimal cooling conditions and package design. Postharvest Biology and Technology. 2017, 126: 67-75.
11. Yuchen Zhang,Meijie Guo,Jun Mei, et al. Effects of Different Postharvest Precooling Treatments on Cold-Storage Quality of Yellow Peach (Amygdalus persica)[J]. Plants, 2022, 11(18).
12. M Zare,H Dehghan,S Yazdanirad, et al. Comparison of the Impact of an Optimized Ice Cooling Vest and a Paraffin Cooling Vest on Physiological and Perceptual Strain[J]. Safety and Health at Work, 2019, 10(2): 219-223.
13. Junjie Yin,Mei Guo,Guishan Liu, et al. Research Progress in Simultaneous Heat and Mass Transfer of Fruits and Vegetables During Precooling[J]. Food Engineering Reviews, 2022, 14(2): 307-327.
14. Zhiwei Zhu,Yi Geng,Da-Wen Sun. Effects of Pressure Reduction Modes on Vacuum Cooling Efficiency and Quality Related Attributes of Different Parts of Pakchoi (Brassica Chinensis L.)[J]. Postharvest Biology and Technology, 2021, 173.
15. Maria A E, Medeiros A J, Henrique N G, et al. Cantaloupe melon (Cucumis melo L.) conservation using hydrocooling. Revista Ceres. 2016, 63(2): 191-197.
16. Garrido Y, Tudela J A, María I G. Comparison of industrial precooling systems for minimally processed baby spinach. Postharvest Biology and Technology. 2015, 102: 1-8.

17. Liang Y, Orathai W, Suan W P, et al. Influence of hydrocooling on browning and quality of litchi cultivar Feizixiao during storage. International Journal of Refrigeration. 2013, 36(3): 1173-1179.
18. Zainal B, Ding P, Ismail I S, et al. Physico-chemical and microstructural characteristics during postharvest storage of hydrocooled rockmelon (Cucumis melo L. reticulatus cv. Glamour). Postharvest Biology and Technology. 2019A, 152: 89-99.
19. Zainal B, Ding P, Ismail I S, et al. H NMR metabolomics profiling unveils the compositional changes of hydro-cooled rockmelon (Cucumis melo L. reticulatus cv glamour) during storage related to in vitro antioxidant activity. Scientia Horticulturae. 2019B, 246(27): 618-633.
20. Tao Z. Difficulties and countermeasures of the circulation of litchi in Guangxi. Management and Technology of Small and Medium Sized Enterprises. 2017, 11(4): 45-46.
21. Chieh Yang,Fang-Wei Lee,Yu-Jung Cheng, et al. Chitosan coating formulated with citric acid and pomelo extract retards pericarp browning and fungal decay to extend shelf life of cold-stored lychee[J]. Scientia Horticulturae, 2023, 310.
22. Gan L, Chen M, Lv E. Effect of different precooling methods on litchi precooling. Modern Agricultural Equipment. 2020, 41(5): 8-13.
23. G Alva,YX Lin,GY Fang. An overview of thermal energy storage systems[J]. Energy, 2018, 144: 341-378.
24. P. McKenna,W.J.N. Turner,D.P. Finn. Thermal energy storage using phase change material: Analysis of partial tank charging and discharging on system performance in a building cooling application[J]. Applied Thermal Engineering, 2021, 198.
25. Jia Y X, Liu Y S, Sun S F, et al. Refrigerating characteristics of ice storage capsule for temperature control of coal mine refuge chamber. Applied Thermal Engineering. 2015, 75: 756-762.
26. Biosca-taronger J, Payá J, López-navarro A, et al. Ice formation modelling around the coils of an ice storage tank[C]//6th European Thermal Sciences Conference, Institute of Physics Publishing, 2012, 395, 2012-01-01.
27. Liu R. Experiment research and numerical simulation of heat pipe ice storage. East China Jiaotong University: Nanchang, 2011.
28. Ye S, Chen G, Chen L, et al. Influence of freezing thickness on heat transfer resistance of ice-on-coil, iceball and metal-cored iceball. Cryogenics. 2001, 6: 62-65.
29. Li P. Study on the heat transfer characteristics of the refrigeration fluoroethane (HFC-161) flow boiling inside tubes. Zhejiang University: Hangzhou, 2013.
30. Wu S M, Fang G Y, Chen Z. Discharging characteristics modeling of cool thermal energy storage system with coil pipes using n-tetradecane as phase change material. Applied Thermal Engineering. 2012, 37: 336-343.
31. Jin W, Lu H. Refrigeration technology. Mechanical Industry Press: Beijing, 2009.
32. Wang H. Estimation of Thermal Properties of Lychee. Journal of Shenzhen Polytechnic. 2006, 3: 23-26.
33. Yang S M, Tao W Q. Heat Transfer. Forth edition. Higher Education Press: Beijing, 2006.
34. Mehmet A E, Aytunç E, Ibrahimdincer. Energy and exergy analyses of an ice-on-coil thermal energy storage system. Energy. 2011, 36(11): 6375-6386.
35. Ogawa N, Kaneko F. Experiment and mathematical model for the heat transfer in water around 4 °C. European Journal of Physics. 2017, 38(2): 1-13.